Free-forced convective boundary-layer flow of a biomagnetic fluid under the action of a localized magnetic field

N.G. Kafoussias, E.E. Tzirtzilakis, and A. Raptis

Abstract: The problem of the two-dimensional steady and laminar free-forced convective boundary-layer flow of a biomagnetic fluid over a semi-infinite vertical plate, under the action of a localized magnetic field, is numerically studied. The dynamic viscosity of the biomagnetic fluid as well as its thermal conductivity is considered to be temperature-dependent whereas the magnetization of the fluid varies linearly with the magnetic field strength. The numerical solution of the coupled and nonlinear system of partial differential equations (resulting after the introduction of appropriate nondimensional variables) with boundary conditions describing the problem under consideration, is obtained by an efficient numerical technique based on the common finite difference method. Numerical calculations were carried out for the case of blood ($Pr = 21$) for different values of the dimensionless parameters entering into the problem, especially for the magnetic parameter Mn and the viscosity–temperature parameter Θ_r. The analysis of the obtained results, presented in figures, shows that the flow field is influenced by the application of the magnetic field, which could be interesting for medical and bioengineering applications.

PACS Nos.: 44.20.+b, 44.25.+f, 44.27.+g, 47.15.Cb, 47.65.Cb, 47.63.−b, 47.90.+a

Résumé : Nous étudions numériquement l'écoulement 2-D stationnaire et laminaire sans force de la couche limite convective d'un fluide biomagnétique sur une plaque verticale semi-infinie en présence d'un champ magnétique local. Nous considérons que la viscosité dynamique et la conductivité thermique du fluide biomagnétique dépendent de la température, alors que la magnétisation du fluide varie linéairement avec l'amplitude du champ magnétique. Une méthode numérique efficace basée sur l'habituelle approche aux différences finies permet d'obtenir la solution numérique du système d'équations aux dérivées partielles couplées et non linéaires, résultant de l'introduction des variables sans dimensions avec conditions limites adaptées au problème considéré. Nous avons fait des calculs pour le sang ($Pr = 21$) pour différentes valeurs des quantités sans dimensions qui entrent dans le problème, spécialement le paramètre de magnétisation Mn et le paramètre de viscosité/température Θ_r. L'analyse des résultats présentés graphiquement montre que le champ d'écoulement est influencé par la présence du champ magnétique, ce qui pourrait devenir intéressant en médecine et en bioingénierie.

[Traduit par la Rédaction]

1. Introduction

Biomagnetic fluid dynamics (BFD) is a relatively new area in fluid dynamics, and during the last decades extensive research work has been done on the fluid dynamics of biological fluids in the presence of magnetic fields. There are many applications for this research in bioengineering and medicine, and the research work in this subject is growing rapidly [1–10].

A biomagnetic fluid is a fluid that exists in a living creature and its flow is influenced by the presence of a magnetic field. The most characteristic biomagnetic fluid is blood, which can be considered as a magnetic fluid because red blood cells contain the hemoglobin molecule, a form of iron oxide, which is present at a uniquely high concentration in mature red blood cells [11, 12]. Blood possesses the property of a diamagnetic material when oxygenated, but is paramagnetic when deoxygenated. The magnetic susceptibility χ of blood is 3.5×10^{-6} and -6.6×10^{-7} for venous and arterial blood, respectively [13, 14].

To examine the flow of a biomagnetic fluid under the action of an applied magnetic field, mathematical models have been developed for BFD. The implementation of these models is based on modified Stokes principles and on the assumption that besides the three thermodynamic variables, i.e., pressure P, density ρ, and temperature T, the biomagnetic fluid behavior is also a function of magnetization M [15].

However, the effect of a magnetic field on pure blood is very weak, and strong magnetic fields are required to affect its flow. Thus, in several biomedical applications, such as magnetic drug targeting, artificially created magnetic nanoparticles are added to blood [16]. In that case, the effect of the magnetic field on blood flow increases dramatically as long as its magnetization M increases several orders of magnitude. Consequently, blood with added magnetic particles, except from paramagnetic or diamagnetic material, can be considered as a ferromagnetic fluid.

Received 6 March 2007. Accepted 24 September 2007. Published on the NRC Research Press Web site at http://cjp.nrc.ca/ on 28 March 2008.

N.G. Kafoussias[1] and E.E. Tzirtzilakis. Department of Mathematics, Section of Applied Analysis, University of Patras, 26 500 Patras, Greece.
A. Raptis. Department of Mathematics, Section of Applied Mathematics and Mechanical Research, University of Ioannina, 453 32 Ioannina, Greece.

[1]Corresponding author (e-mail: nikaf@math.upatras.gr.) (On leave of absence).

 doi: 10.1139/P07-166

The first formulation of BFD for the investigation of the flow of a biofluid under the influence of an applied magnetic field (biomagnetic fluid flow) was developed by Haik et al. [15]. According to this formulation, the biomagnetic fluid is actually considered to possess the magnetic properties of blood. The blood in that BFD formulation is treated as a homogeneous, Newtonian, electrically nonconducting magnetic fluid. Clearly, the mathematical model of Haik et al. [15] is valid for laminar blood flow in large vessels where the Newtonian behavior is a good approximation [17, 18]. Moreover, the BFD model is actually based on ferro hydrodynamics (FHD) [19–26], which deals with no induced electric current and considers that the flow is affected by the magnetization of the fluid in the magnetic field [13, 15, 16].

The two classical problems in fluid mechanics, namely, the Blasius boundary-layer flow along a flat plate and the stagnation point flow, were extended for a saturated ferro fluid under the combined influence of thermal and magnetic field gradients by Neuringer [26]. The flow of a viscous fluid past a linearly stretching surface in otherwise quiescent surroundings was first considered by Crane [27] for a Newtonian fluid. The same problem was extended to fluids obeying non-Newtonian constitutive equations such as viscoelastic [28], micropolar [29], and inelastic power-law fluids [30]. Some of these cases were later extended to include the effect of a uniform transverse magnetic field on the motion of an electrically conducting fluid driven by a stretching sheet [31–33].

Crane's problem was extended by Andersson and Valnes [34], who studied the influence of a magnetic field due to a magnetic dipole on shear-driven motion (flow over a stretching sheet) of a viscous nonconducting ferro fluid. The fluid flow was formulated as a five-parameter problem, and the influence of the magneto-thermo-mechanical coupling was explored numerically. It was concluded from this work that the primary effect of the magnetic field was to decelerate the fluid motion compared with the hydrodynamic case. In their study, they also considered that the magneto-thermo-mechanical coupling is completely described by assuming that the applied magnetic field $\boldsymbol{H}$ is sufficiently strong to saturate the ferro fluid, and that the variation of magnetization M with temperature T can be approximated by a linear equation of state.

Tzirtzilakis and Kafoussias [35] extended the problem studied by Andersson and Valnes [34] by assuming that the magneto-thermo-mechanical coupling is not described by a linear function of temperature difference but by a nonlinear one, the expression of which was used by Arrot et al. [36]. A comparative study with the Andersson and Valnes work showed the importance of the nonlinear variation of magnetization with temperature.

Loukopoulos and Tzirtzilakis [37] studied the biomagnetic channel flow in a spatially varying magnetic field, assuming that the magnetization M of the fluid is varying linearly with fluid temperature T and magnetic field strength H. Tzirtzilakis et al. [38] studied the laminar, incompressible, three-dimensional, fully developed viscous flow of a nonconducting biomagnetic fluid in an impermeable walled rectangular duct in the presence of an applied magnetic field. It was assumed in that work that the magnetic field strength was strong enough to saturate the biofluid and that the magnetization was given as a function of the magnetic field strength. The system of partial differential equations, resulting after the introduction of appropriate nondimensional variables, was solved by applying an efficient numerical technique based on a pressure-linked pseudotransient method on a common grid [38].

Finally, Tzirtzilakis et al. [39] studied the fundamental problem of the turbulent flow of a biomagnetic fluid (blood) between two parallel plates under the action of a localized magnetic field. The blood was considered to be an electrically conducting, incompressible, and Newtonian fluid and its flow was considered to be steady, two-dimensional, and turbulent. The turbulent flow was described by the Reynolds-averaged Navier–Stokes (RANS) equations. For the numerical solution of this problem, which is described by a system of coupled nonlinear partial differential equations (PDEs), with appropriate boundary conditions, the stream function – vorticity formulation was used. For the eddy-kinematic viscosity, the low-Reynolds-number $k - \varepsilon$ turbulence model was adopted. The solution of the problem, for different values of the dimensionless parameter entering into it, was obtained by developing and applying an efficient numerical technique based on a finite differences scheme.

Another classical problem in fluid mechanics is the free-forced convective boundary-layer flow of a viscous incompressible fluid over a vertical hot plate surface. However, as far as could be investigated, such a problem for a biomagnetic fluid (ferro fluid) and under the action of a localized magnetic field has not yet been studied.

Hence, the aim of the present work is the numerical investigation of the two-dimensional steady and laminar free-forced convective boundary-layer flow of a biomagnetic fluid over a semi-infinite vertical hot plate under the action of a localized magnetic field. The magnetic field $\boldsymbol{H}$ is considered to be of sufficient strength to saturate the biomagnetic fluid and the magnetization of the fluid is considered to be a linear function of the magnetic field strength. For the mathematical formulation of the problem, which is presented in Sect. 2, the variation of dynamic viscosity μ and of the thermal conductivity k with temperature T is taken into account.

The numerical solution of the coupled nonlinear system of PDEs with its boundary conditions, describing the problem under consideration, is obtained by an efficient numerical solution technique presented in Sect. 3. Finally, numerical results for the fundamental quantities of the flow field, such as the velocity and temperature profiles and the skin friction and heat transfer coefficients, are presented in Sect. 4 for the case of blood ($Pr = 21.0$) for different values of the dimensionless parameters entering into the problem, namely, the magnetic parameter Mn, the viscosity–temperature parameter Θ_r, and for the value of the thermal conductivity parameter S^* equal to 0.14. The analysis of the results obtained indicates that the application of a magnetic field in such a flow of a biomagnetic fluid could be interesting and useful for medical and bioengineering applications.

2. Mathematical formulation of the problem

The steady, laminar, free-forced convective boundary-layer flow of a viscous incompressible and homogeneous biomagnetic fluid along a semi-infinite vertical flat plate is considered.

According to the initial biomagnetic fluid dynamics model of Haik et al., blood is considered an electrically nonconducting

fluid, and several studies have been made adopting this simplification [6, 9, 13, 15, 22, 35, 37, 38, 40]. However, blood is, in reality, electrically conducting. A newer version of the biomagnetic fluid dynamics that takes into account the electrical conductivity of blood has been presented in ref. 41. In this study, an extensive investigation has been performed to determine whether the electrical conductivity must be taken into account or not. According to this study, the electrical conductivity can be ignored in the following cases:

(*i*) when the magnetic field gradient is sharp enough so that the force due to magnetization prevails in the flow field,

(*ii*) the absolute value of the adopted magnetic field flux is at most about 2 T, and

(*iii*) in several biomedical applications where artificially created nanoparticles are added to the fluid.

As mentioned in the Introduction, it is a common practice in biomechanical applications, such as drug delivery, to add artificially created nanoparticles [6, 13, 16, 22]. In this case, blood is treated as a ferromagnetic fluid, and magnetic field strengths of 0.1 or 0.5 T are sufficiently strong to saturate the magnetic fluid. Consequently, the magnetic field is much less than 2 T, and in those cases of biomedical applications the electrical conductivity of the fluid can be also considered negligible. In the current study, the fluid is considered to behave like an electrically nonconducting magnetic fluid as with biomechanical applications.

In a Cartesian coordinate system *Oxyz*, the plate is located at,

$$y = 0, \qquad 0 \le x, \qquad -\infty < z < +\infty$$

The plate is parallel to the free stream of the biomagnetic fluid, flowing with velocity u_∞ in the positive x direction. The temperature T_w of the wall plate is uniform and constant and greater than the free-stream temperature T_∞. It is also assumed that the free-stream velocity u_∞, parallel to the vertical plate and in the positive x direction, is constant. The flow is subject to the action of a localized magnetic field $\boldsymbol{H}$ of sufficient strength to saturate the biomagnetic fluid. The magnetic field is generated by an electric current with intensity I going through an infinitely thin wire placed parallel to the plate (to the z axis) and at a distance a from the origin of the Cartesian coordinate system *Oxyz* and at a distance b below the plate (Fig. 1). So, the position of this wire is,

$$(x_0, y_0, z) = (a, b, z), \quad a > 0, \quad b < 0, \quad z \in \Re$$

The magnitude $\|\boldsymbol{H}\|$ of the magnetic field strength is given by,

$$\|\boldsymbol{H}\| = H(x, y) = \frac{I}{2\pi} \frac{1}{\left[(x-a)^2 + (y-b)^2\right]^{1/2}} \tag{1}$$

Fluid properties variations with temperature are limited to density, dynamic viscosity, and thermal conductivity, with the density variation taken into account only insofar as it effects the buoyancy term in the momentum equation (Boussinesq approximation).

Under these assumptions, the two-dimensional boundary-layer equations in the *Oxy*-plane for the free-forced convective

Fig. 1. Schematic representation of the flow field.

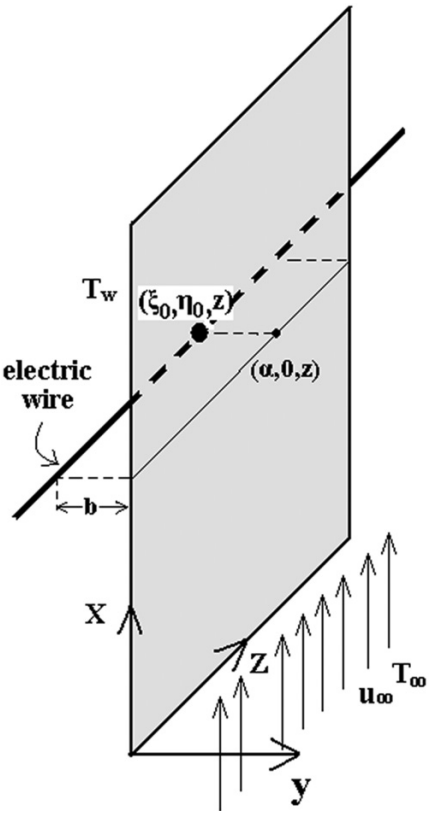

flow of the biomagnetic fluid past the semi-infinite vertical plate are,

$$\frac{\partial u}{\partial x} + \frac{\partial \upsilon}{\partial y} = 0 \tag{2}$$

$$u\frac{\partial u}{\partial x} + \upsilon\frac{\partial u}{\partial y} = \frac{1}{\rho_\infty}\frac{\partial}{\partial y}\left(\mu\frac{\partial u}{\partial y}\right) + g\beta(T - T_\infty) \pm \frac{\mu_o}{\rho_\infty} M \frac{\partial H}{\partial x} \tag{3}$$

$$u\frac{\partial T}{\partial x} + \upsilon\frac{\partial T}{\partial y} - \frac{\mu_o}{\rho_\infty c_p} T \frac{\partial M}{\partial T}\left(u\frac{\partial H}{\partial x} + \upsilon\frac{\partial H}{\partial y}\right) = \frac{1}{\rho_\infty c_p}\frac{\partial}{\partial y}\left(k\frac{\partial T}{\partial y}\right) \tag{4}$$

The boundary conditions of the problem are

$$y = 0: \quad u = 0, \quad \upsilon = 0, \quad T = T_w \tag{5}$$

$$y \to \infty: \quad u = u_\infty, \quad T = T_\infty \tag{6}$$

It is known that in an equilibrium situation, the magnetization property is generally determined by the fluid temperature T, fluid density ρ, and magnetic field strength H. Various equations describing the dependence of magnetization M on these quantities can be found in refs. 21–27 and in refs. 35–42. The simplest is a linear equation involving only the magnetic field strength H, referred to also in refs. 22, 25, 38, 41, and 43, that is,

$$\boldsymbol{M} = \chi \boldsymbol{H} \tag{7}$$

In (7), χ is the magnetic susceptibility of the fluid and is considered to be a constant. Equation (7) constitutes a good approximation, as experiments show [13], because especially for blood, the magnetization does not seem to be affected by the temperature variations in the flow field. It is worth remembering here that the magnetic susceptibility χ takes positive values for paramagnetic materials and negative values for diamagnetic ones.

Expression (7) is adopted for the physical problem under consideration. Under the earlier assumption, the magnetization M is independent of fluid temperature T, and hence the last term on the left-hand side of the energy equation (4),

$$\frac{\mu_o}{\rho_\infty c_\mathrm{p}} T \frac{\partial M}{\partial T}\left(u\frac{\partial H}{\partial x}+\upsilon\frac{\partial H}{\partial y}\right)$$

representing the thermal power per unit volume due to the magneto-caloric effect, is equal to zero.

On the other hand, the term

$$\pm\frac{\mu_o}{\rho_\infty} M\frac{\partial H}{\partial x} = \pm\frac{\mu_o}{\rho_\infty}\chi H\frac{\partial H}{\partial x}$$

in (3), represents the component of the magnetic force, per unit volume, in the x direction and depends on the existence of the magnetic gradient and on the magnetic susceptibility χ. The sign of the magnetic body force term denotes that the fluid is attracted or repelled by the application of the magnetic field. The attraction or repulsion of the fluid could be possibly achieved artificially by proper construction of magnetic nanoparticles for biomedical applications. Moreover, attraction or repulsion is observed in pure blood since blood possesses the properties of a diamagnetic material when oxygenated ($\chi = -6.6\times10^{-7}$) and of a paramagnetic material when deoxygenated ($\chi = 3.5\times 10^{-6}$) [12–14]. A discussion of and results following from the change of sign of the magnetic body force term can be also found in ref. 41. Consequently, the positive sign corresponds to the case in which the fluid is considered to be paramagnetic ($\chi > 0$), whereas the minus sign corresponds to the case in which the fluid is considered to be diamagnetic ($\chi < 0$).

The mathematical analysis of the problem is simplified by introducing the following dimensionless coordinates of transformation:

$$\xi(x) = \frac{Gr_x}{Re_x^2} = cx$$
$$\eta(x,y) = Re_x^{1/2}\frac{y}{x}, \quad y \geq 0, \quad x > 0 \tag{8}$$

In (8), Gr_x and Re_x are the local Grashof and local Reynolds numbers, respectively, given by the expressions,

$$Gr_\chi = \frac{g\beta(T_\mathrm{w}-T_\infty)x^3}{v_\infty^2}, \qquad Re_x = \frac{xu_\infty}{v_\infty} \tag{9}$$

$$c = \frac{g\beta(T_\mathrm{w}-T_\infty)}{u_\infty^2} \tag{10}$$

and ν_∞ is the free-stream kinematic viscosity ($\nu_\infty = \mu_\infty/\rho_\infty$).

In addition, a reduced stream function $F(\xi,\eta)$ and a dimensionless temperature $\Theta(\xi,\eta)$ are defined as follows:

$$F(\xi,\eta) = \frac{\Psi(x,y)}{\nu_\infty Re_x^{1/2}}$$
$$\Theta(\xi,\eta) = \frac{T-T_\infty}{T_\mathrm{w}-T_\infty} \tag{11}$$

The function $\Psi(x,y)$ is the stream function that ensures that the continuity equation (2), is automatically satisfied so that,

$$(u,\upsilon) = \left(\frac{\partial\Psi}{\partial y}, -\frac{\partial\Psi}{\partial x}\right) \tag{12}$$

For a viscous fluid, Ling and Dybbs [44] suggested a viscosity dependence on temperature T of the form,

$$\mu = \frac{\mu_\infty}{1+\gamma(T-T_\infty)} \tag{13}$$

So, the viscosity of the fluid is an inverse linear function of temperature T.

Equation (13) can be rewritten as

$$\frac{1}{\mu} = \alpha(T-T_\mathrm{r}) \quad \text{where} \quad \alpha = \frac{\gamma}{\mu_\infty}, \quad T_\mathrm{r} = T_\infty - \frac{1}{\gamma} \tag{14}$$

In (14), both α and T_r are constants whose values depend on the reference state, and γ is a thermal property of the fluid.

The dimensionless temperature Θ can be written now as,

$$\Theta = \frac{T-T_\mathrm{r}}{T_\mathrm{w}-T_\infty} + \Theta_\mathrm{r} \tag{15}$$

where

$$\Theta_\mathrm{r} = \frac{T_\mathrm{r}-T_\infty}{T_\mathrm{w}-T_\infty} = -\frac{1}{\gamma\,(T_\mathrm{w}-T_\infty)} = \text{const.} \tag{16}$$

and its value is determined by the viscosity and temperature characteristics of the fluid and the operating temperature difference $\Delta T = T_\mathrm{w} - T_\infty$.

It is also assumed that the fluid thermal conductivity k is expressed by a linear function of temperature of the form [45],

$$k = k_\infty\,[1 + s\,(T-T_\infty)] \tag{17}$$

where s is a constant dependent on the nature of the fluid, and k_∞ is the ambient fluid thermal conductivity. This form can also be rewritten as

$$k = k_\infty\left(1+S^*\Theta\right) \tag{18}$$

where

$$S^* = s\,(T_\mathrm{w}-T_\infty) \tag{19}$$

is the thermal-conductivity parameter [46].

The substitution of (1) and of (7)–(18) into (3) and (4) gives the following system:

$$F''' - \frac{1}{2}F\frac{\Theta-\Theta_r}{\Theta_r}F'' - \frac{\Theta'}{\Theta-\Theta_r}F'' - \xi\,(\Theta-\Theta_r)\,\frac{\Theta}{\Theta_r} = \xi\left\{\frac{\partial F}{\partial \xi}F'' - F'\frac{\partial F'}{\partial \xi}\right\}\frac{\Theta-\Theta_r}{\Theta_r} \mp RMn\frac{\Theta-\Theta_r}{\Theta_r} \times \frac{\xi(\xi-ac)}{\left[(\xi-ac)^2+(d\sqrt{\xi}\eta-cb)^2\right]^2} \quad (20)$$

$$\frac{1}{Pr}\left(1+S^*\Theta\right)\Theta'' + \left(\frac{1}{2}F + \frac{1}{Pr}S^*\Theta'\right)\Theta' + \xi\frac{\partial F}{\partial \xi}\Theta' = \xi F'\frac{\partial \Theta}{\partial \xi} \quad (21)$$

where $Pr = \mu_\infty c_p/k_\infty$ is the Prandtl number, primes denote partial differentiation with respect to the variable η, $d = \sqrt{c\nu_\infty/u_\infty}$ and RMn is defined as $RMn = Mn(cb)^2$. In the above relations Mn is the magnetic parameter or magnetic number. It expresses the ratio of the magnetic forces to the inertia forces (per unit volume) and it is defined as $Mn = M_0B_0/\rho_\infty u_\infty^2$, where $M_0 = \chi H_0$, $B_0 = \mu_0 H_0$, and H_0 is the magnetic field strength at the point $(x_0, y_0, z_0) = (\alpha, 0, z)$. It is worth noting here that in the case where $Mn = 0$ and $S^* = 0$, the problem under consideration becomes similar to that presented in ref. 47 and solved by a different numerical technique.

Finally, the boundary conditions (5) and (6) become,

$$\eta = 0: \quad F' = 0, \quad F = 0, \quad \Theta = 1 \quad (22)$$

$$\eta \to \infty: \quad F' = 1, \quad \Theta = 0 \quad (23)$$

The dimensionless parameters entering into the problem under consideration and described by the system of (20) and (21), are the Prandtl number Pr, the magnetic number Mn, the viscosity–temperature parameter Θ_r, and the thermal–conductivity parameter S^*.

3. Numerical solution

The physical problem under consideration is described by the system of nonlinear equations (20) and (21), subject to the boundary conditions (22) and (23). The unknown functions are the dimensionless stream function $F(\xi, \eta)$ (or the velocity profile $F'(\xi, \eta)$) and the dimensionless temperature $\Theta(\xi, \eta)$. The primes denote differentiation with respect to η, and the dimensionless parameters entering into the system are the Prandtl number Pr, the viscosity–temperature parameter Θ_r, the thermal–conductivity parameter S^*, and the magnetic parameter Mn. The system of equations (20) and (21) is of parabolic type and can be solved by several numerical methods.

The applied numerical scheme consists in proceeding in the ξ direction, i.e., calculating unknown profiles at ξ_{i+1} when the same profiles at ξ_i are known. The process starts at $\xi = 0$ where (20) and (21) reduce to,

$$F''' - \frac{1}{2}F\frac{\Theta-\Theta_r}{\Theta_r}F'' - \frac{\Theta'}{\Theta-\Theta_r}F'' = 0 \quad (24)$$

$$\frac{1}{Pr}\left(1+S^*\Theta\right)\Theta'' + \left(\frac{1}{2}F + \frac{1}{Pr}S^*\Theta'\right)\Theta' = 0 \quad (25)$$

The boundary conditions for these equations are the same as those of the complete system of equations. The numerical solution of the above system is easily obtained by applying the efficient numerical technique described in detail in ref. 48.

To proceed from ξ_i to ξ_{i+1}, the equations are discretized at $\xi_{i+1/2}$ and η_j with central differences for the first- and second-order η-derivatives, averaged at ξ_i and ξ_{i+1}, and backward differences for first-order ξ-derivatives. This Crank–Nicolson-type numerical scheme is $O(\Delta\xi^2)$ and $O(\Delta\eta^2)$ and is implemented on a uniform $\xi - \eta$ grid. Once an estimate of the unknown $F'_{i+1,j}$ is available, the energy equation (21) provides an estimate for $\Theta_{i+1,j}$ using a fast tridiagonal scheme. This profile is fed into the momentum equation (20), which is solved by iterating on a tridiagonal equation and a new estimate of $F'_{i+1,j}$ is obtained. The process is repeated until the velocity profile at ξ_{i+1} does not exhibit appreciable variations. Numerical infinity for η, viz. $\eta_\infty(= 10.0)$, must be adjusted according to the final ξ station, up to which the boundary-layer calculations are performed. The steps $\Delta\xi(= 0.02)$ and $\Delta\eta(= 0.05)$ are adjusted experimentally until the results obtained are not numerically sensitive beyond the desired accuracy. Derivatives are calculated via a forward differences Newton scheme. The above numerical solution is similar to that described in refs. 49 and 50 and has been proved to be quite simple and efficient.

It has also been generally recognized that the governing parameter for such a flow type as in the current work is the dimensionless ratio $\xi(x) = Gr_x/Re_x^2$, where Gr_x and Re_x are the local Grashof and Reynolds numbers, respectively. Forced-convection exists as a limit when ξ goes to zero, which occurs at the leading edge, and the free-convection limit can be reached if ξ becomes large. The dimensionless parameter ξ, in mixed convection problems, represents the ratio of buoyancy forces to the inertial forces inside the boundary layer. When ξ is of the order of unity, both buoyancy and inertia forces can contribute to the flow. With increasing ξ, however, the effect of buoyancy forces increases, and when ξ is large it is better to change the similarity variables η and Ψ to those for pure natural convection [51]. For the applications in the current work, the maximum value of ξ (ξ_{final}) has been chosen to be equal to 0.5 ($x_{final} = 0.76$).

In a single experiment, when the fluid and temperature parameters are fixed, ξ may be regarded as a dimensionless distance along the plate from the leading edge, whereas changing the fluid and temperature parameters merely alters the scale of the distance relative to the actual distance x. Near the leading edge, $\xi \ll 1$ and forced convection dominates. As ξ increases ($\xi \sim 1$), the fluid moves into the mixed convection regime and subsequently into a free convection dominated flow ($\xi \gg 1$).

On the other hand, in combined, natural and forced convection problems for fluids with $Pr > 1$, the scale criterion for transition from natural to forced convection is the ratio r de-

fined as [52],

$$r = \frac{Ra_x^{1/4}}{Re_x^{1/2} Pr^{1/3}} \tag{26}$$

where Ra_x is the local Rayleigh number defined as $Ra_x = Gr_x Pr$. When $r > O(1)$ the flow is dominated by the free convection currents, whereas when $r < O(1)$ the flow can be characterized as forced convection flow. For the applications in the current work and for the maximum value of $\xi = \xi_{\text{final}} = 0.5$, r was found equal to 0.65, and under these circumstances the flow can be considered forced rather than natural.

4. Results and discussion

To study the effects of the various parameters of the problem under consideration on the flow of a biomagnetic fluid, the following assumptions were adopted.

The biomagnetic fluid was considered to be human blood. The temperature T_w of the vertical plate as well as the fluid temperature T_∞ in the free stream were considered to be constants ($T_w = 318$ K (45 °C) and $T_\infty = 288$ K (15 °C)). So, the temperature difference $\Delta T = T_w - T_\infty$ was equal to 30 K. The fluid density ρ_∞ at the free steam and the free stream velocity u_∞ of the biomagnetic fluid were taken as $\rho_\infty = 1050\,\text{kg m}^{-3}$ and $u_\infty = 0.28\,\text{m s}^{-1}$, respectively. This velocity corresponds to a possible velocity of blood in a human artery [53]. The coefficient of thermal expansion β of the fluid was taken as $\beta = 0.18 \times 10^{-3}\,\text{K}^{-1}$ [51] and the acceleration due to gravity as $g = 9.81\,\text{m s}^{-2}$.

Although the viscosity μ, the specific heat under constant pressure c_p, and the thermal conductivity k of any fluid, and hence of the blood, are temperature dependent, the Prandtl number $Pr = \mu_\infty c_p / k_\infty$ can be considered constant. The values of μ, c_p, and k are $3.2 \times 10^{-3}\,\text{kg m}^{-1}\,\text{s}^{-1}$, $4 \times 10^3\,\text{J kg}^{-1}\,\text{K}^{-1}$, and $0.6\,\text{J m}^{-1}\,\text{s}^{-1}\,\text{K}^{-1}$, respectively, and thus $Pr = 21.0$ [54, 55]. Under these assumptions, the constant c defined in (10) takes the value $c = 0.662$, and assuming that the electric wire is placed at the position $(x_0, y_0) = (\alpha, b) = (0.50, -0.20)$, the position of the wire in the transformed and dimensionless coordinate system $O\xi\eta$ is $(\xi_0, \eta_0) = (0.331, -85.73)$.

For the values of the viscosity–temperature parameter Θ_r, it is worth remembering here that in the case where the temperature difference $\Delta T = T_w - T_\infty$ is positive, it takes on negative values for liquids, and these values are determined by the viscosity and temperature characteristics of the fluid, the reference temperature T_r, and the operating temperature difference ΔT [47, 56]. In the case under consideration, the values of Θ_r were taken to be equal to -0.40, -0.50, and -0.60.

On the other hand, for the considered temperature difference, the value of the thermal conductivity parameter S^* was taken as $S^* = 0.14$, which corresponds to human blood of haematocrit value ϕ. The value of ϕ was taken equal to 0.45 [46]. Finally, the values of the magnetic parameter Mn were taken equal to 0.0, 0.20, 0.30, 0.40, and 0.60. Moreover, in biomagnetic applications the magnetic susceptibility can be increased artificially two or three orders of magnitude by the addition of magnetic nanoparticles [16, 41]. From experiments it is also known that the saturation magnetization of blood is $40\,\text{A m}^{-1}$ [6, 13, 15]. This value is attained for pure blood for a strong magnetic field of about 7 T. For the present work, the case of a biomedical application fluid flow can be treated as one where additional magnetic nanoparticles have been added. These nanoparticles are assumed to be in sufficient concentration so that the magnetization of $40\,\text{A m}^{-1}$ is attained for a magnetic field strength induction of 1 T. For $Mn = 0.6$ this results in $\rho_\infty = 1050\,\text{kg m}^{-3}$, $u_\infty = 0.28\,\text{m s}^{-1}$, $Mo = 40\,\text{A m}^{-1}$, and Bo of about 1.2 T. For this value of Bo, the assumption that the electrical conductivity of blood is considered negligible is valid. The case $Mn = 0.0$ corresponds to the flow of blood in the absence of a magnetic field.

Under these assumptions the results obtained for the dimensionless quantities of the velocity field $F'(\xi, \eta)$, temperature field $\Theta(\xi, \eta)$, skin friction coefficient C_{f_x}, and Nusselt number Nu_x are presented in Figs. 2–17, accompanied by a comprehensive analysis. It should be noted here that the skin friction coefficient C_f and the Nusselt number Nu are defined by the expressions [51],

$$C_f = \frac{\tau_w}{\rho_\infty u_\infty^2 / 2} \tag{27}$$

and

$$Nu = \frac{x q_w}{k(T_w - T_\infty)} \tag{28}$$

respectively.

In (27) and (28), τ_w is given by,

$$\tau_w = \left(\frac{\mu \partial u}{\partial y} \right)_{y=0} \tag{29}$$

and

$$q_w = -k \left(\frac{\partial T}{\partial y} \right)_{y=0} \tag{30}$$

Using (8) and (11)–(18) in (29) and (30), the corresponding dimensionless quantities C_{f_x} and Nu_x can be written as

$$C_{f_x} = C_f Re_x^{1/2} = \frac{2\Theta_r}{\Theta_r - 1} F''(\xi, 0) \tag{31}$$

and

$$Nu_x = Nu Re_x^{-1/2} = -\Theta'(\xi, 0) \tag{32}$$

Figure 2 shows the variations of the dimensionless skin friction coefficient C_{f_x} against the dimensionless distance ξ for $\Theta_r = -0.50$ and for different values of the magnetic number Mn, whereas the corresponding variations for the dimensionless heat transfer coefficient (Nusselt number) Nu_x, are shown in Fig. 3. Both quantities increase almost linearly with ξ in the absence of a magnetic field ($Mn = 0.0$). However, in the presence of a magnetic field, both quantities are influenced by its presence and especially in the region where the magnetic source is located ($\xi = 0.331$), and this influence is more evident for large values of the magnetic number Mn. It is remarkable that C_{f_x} and Nu_x increases rapidly with the dimensionless distance ξ from the leading edge of the vertical plate, taking their maximum value in the region where the wire is placed ($\xi \sim 0.3$). A little farther downstream, a corresponding decrease takes place up to the point where minimum values are reached ($\xi \sim 0.46$).

Fig. 2. Variations of the dimensionless skin friction coefficient C_{f_x} with the dimensionless distance ξ, for different values of the magnetic number Mn.

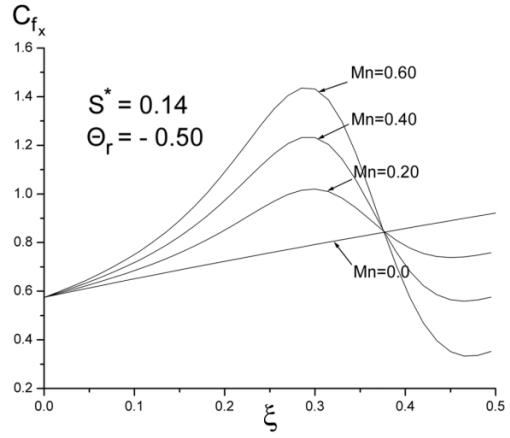

Fig. 3. Variations of the dimensionless Nusselt number Nu_x with the dimensionless distance ξ for different values of the magnetic number Mn.

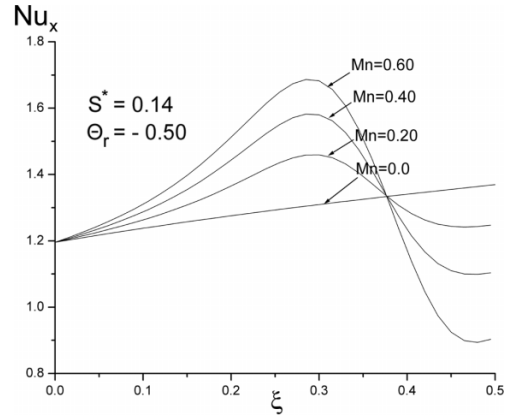

Fig. 4. Variations of the dimensionless skin friction coefficient C_{f_x} with the dimensionless distance ξ for different values of the viscosity–temperature parameter Θ_r.

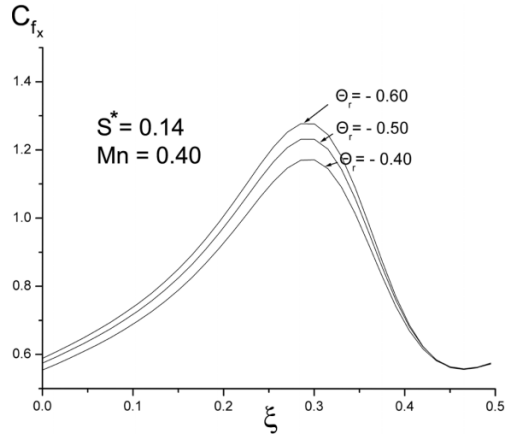

After that point, C_{f_x} and Nu_x increase, but their values remain lower than the corresponding ones in the absence of the magnetic field.

The variation of the various quantities described earlier when $Mn = 0.40$ and for different values of the viscosity–temperature parameter Θ_r are shown in Figs. 4 and 5, respectively. It should

Fig. 5. Variations of the dimensionless Nusselt number Nu_x with the dimensionless distance ξ for different values of the viscosity–temperature parameter Θ_r.

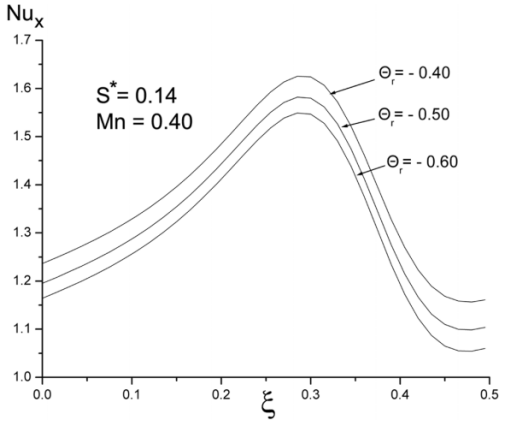

be here that when $|\Theta_r|$ is large, the viscosity variation in the boundary layer is negligible, but as $\Theta_r \to 0^-$, the viscosity variation becomes increasingly significant [47, 56]. From Figs. 4 and 5, it is concluded that the effect of increasing the sensitivity of the viscosity to temperature through the parameter Θ_r is different for C_{f_x} and Nu_x. The skin friction coefficient is increased everywhere as $|\Theta_r|$ increases, whereas the Nusselt number decreases as $|\Theta_r|$ increases. It is worth noting, however, that for large values of ξ, C_{f_x} is not influenced by the variation of the viscosity–temperature parameter Θ_r.

Figures 6 and 7 show the variations of the dimensionless velocity and temperature profiles, respectively, against the dimensionless distance η, normal to the plate, for $Mn = 0.40$, $\Theta_r = -0.50$ and at different locations ξ along the vertical plate. It is concluded that as ξ increases from 0.0 to 0.36, the fluid dimensionless velocity component $F'(\xi, \eta)$, parallel to the plate and inside the boundary layer, increases from zero on the plate to its limited value one at the free stream. It is also observed that near the leading edge of the plate ($\xi = 0.0$ or $\xi = 0.12$) forced convection dominates, but as ξ increases ($\xi = 0.24$ or $\xi = 0.36$) the fluid moves into a mixed convection regime and subsequently into a free convection dominated flow. As the buoyancy acts in the direction of the free stream, the velocity within the boundary layer can exceed the free-stream value $F'(\xi, \infty) = 1$ representing an overshoot ($F'(\xi, \eta) > 1$). On the other hand, as ξ increases, the dimensionless temperature $\Theta(\xi, \eta)$ inside the thermal boundary layer (Fig. 7) decreases, but this is true only for values of $\xi < \xi_0$. At $\xi = 0.36 (> \xi_0)$, the dimensionless temperature for every η is greater than the corresponding one at $\xi = 0.24$, and this can be easily interpreted by taking into account the variation of the heat transfer coefficient (Nusselt number) against ξ, already presented in Fig. 3.

The variations of $F'(\xi, \eta)$ and $\Theta(\xi, \eta)$ for $\Theta_r = -0.50$, $\xi = 0.18$ and 0.36 and for different values of the magnetic number Mn are presented in Figs. 8 and 9, respectively. The corresponding variations of the profiles for $Mn = 0.40$ and for different values of the viscosity–temperature parameter Θ_r are presented in Figs. 10 and 11. From Figs. 8 and 9 it is concluded that for every value of ξ as the electric current intensity (or the magnetic number Mn) increases, the velocity profile increases whereas the temperature profile decreases. These profiles present exactly the same dependence on the viscosity–temperature parameter Θ_r as well, and this is evident in Figs. 10 and 11.

Fig. 6. Variations of the dimensionless velocity profile $F'(\xi, \eta)$ with the dimensionless distance η at different locations ξ along the vertical plate.

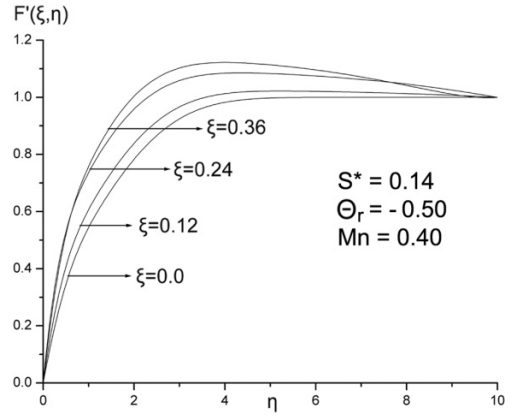

Fig. 7. Variations of the dimensionless temperature profile $\Theta(\xi, \eta)$ with the dimensionless distance η at different locations ξ along the vertical plate.

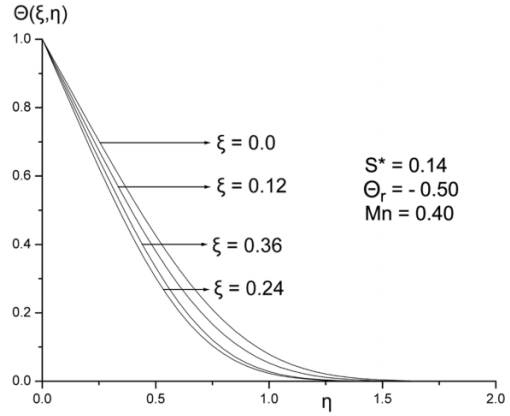

Fig. 8. Variations of the dimensionless velocity profile $F'(\xi, \eta)$ with the dimensionless distance η at different locations ξ along the vertical plate and for different values of the magnetic number Mn.

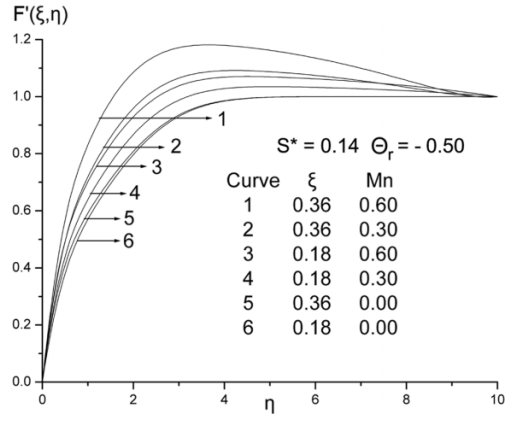

The variations of the skin friction coefficient C_{f_x} against ξ for a positive and negative values of the magnetic parameter Mn and for $Mn = 0.0$ are presented in Fig. 12. It is observed that when $Mn = -0.40$, C_{f_x} takes its minimum value at a value of ξ that is just before the point $\xi = \xi_0$ and before the point where C_{f_x} takes its maximum value for $Mn = 0.40$. It

Fig. 9. Variations of the dimensionless temperature profile $\Theta(\xi, \eta)$ with the dimensionless distance η at different locations ξ along the vertical plate and for different values of the magnetic number Mn.

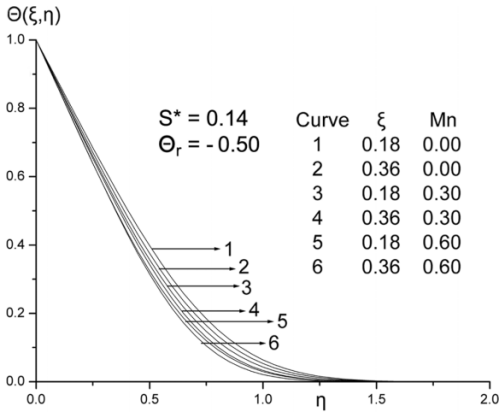

Fig. 10. Variations of the dimensionless velocity profile $F'(\xi, \eta)$ with the dimensionless distance η at different locations ξ along the vertical plate and for different values of the viscosity–temperature parameter Θ_r.

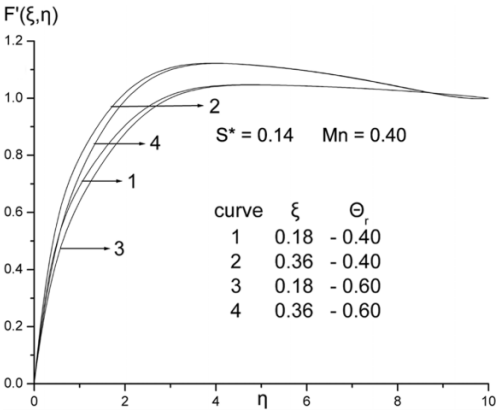

Fig. 11. Variations of the dimensionless temperature profile $\Theta(\xi, \eta)$ with the dimensionless distance η at different locations ξ along the vertical plate and for different values of the viscosity–temperature parameter Θ_r.

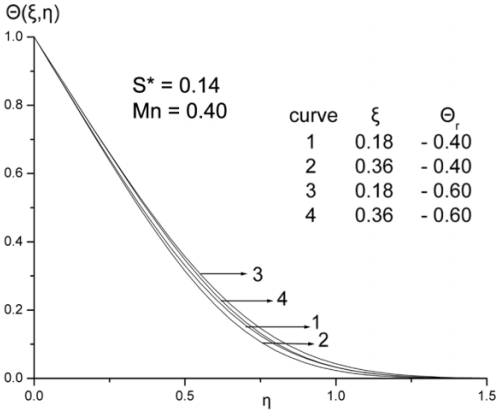

is also remarkable that at this point ξ ($\xi \simeq 0.28$), the difference $((C_{f_x})_{Mn=0.0} - (C_{f_x})_{Mn=-0.40})$ is greater than the corresponding one $((C_{f_x})_{Mn=0.40} - (C_{f_x})_{Mn=0.0})$. Similar behavior is shown in the variations of Nu_x presented in Fig. 13.

Fig. 12. Variations of the dimensionless skin friction coefficient C_{f_x}, with the dimensionless distance ξ, for zero, positive and negative values of the magnetic number Mn.

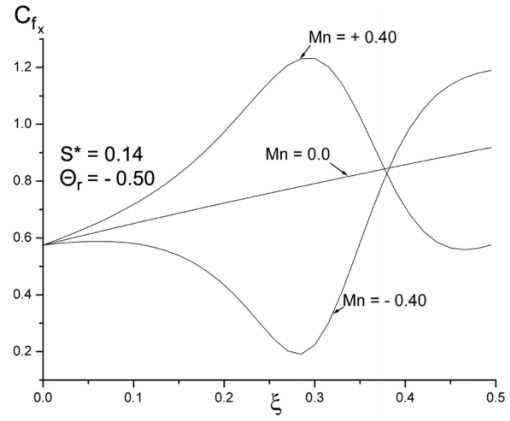

Fig. 13. Variations of the dimensionless Nusselt number Nu_x, with the dimensionless distanceξ, for zero, positive and negative values of the magnetic number Mn.

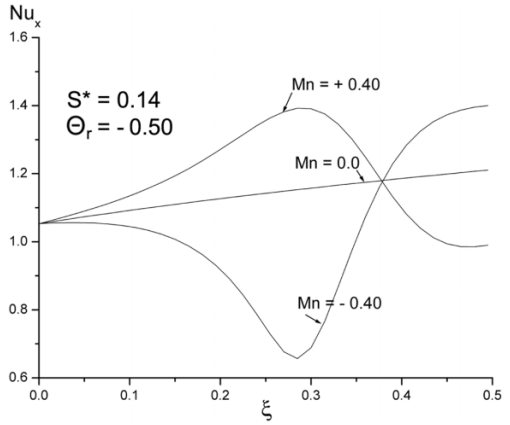

The variations of the dimensionless velocity profiles $F'(\xi, \eta)$ and temperature profiles $\Theta(\xi, \eta)$ for $\xi = 0.24$, $\Theta_r = -0.50$, and for $Mn = 0.0$ and ± 0.40, are presented in Figs. 14 and 15. It is also remarkable here that the influence of the localized magnetic field on both these fields is greater for $Mn < 0$ than for $Mn > 0$. This is due to the fact that in the case $Mn < 0$, the magnetic force per unit volume, which acts now in the negative x direction, is opposed to the action of the buoyancy force that acts in the positive x direction. Quantitatively, when $\eta = 2.0$ and Mn increases from 0.0 to +0.40, the percentage change (increment) of the velocity profile $F'(\xi, \eta)$ is 19.21%. On the other hand, when $\eta = 2.0$ and when Mn is changed from 0.0 to −0.40, the percentage change (decrement) of $F'(\xi, \eta)$ is 29.19%. The corresponding changes for the temperature profile when $\eta = 0.75$, are 40.07% (decrement) and 98.5% (increment), respectively.

Finally, the numerical investigation of the current problem showed that the velocity field and the skin friction coefficient are not appreciably influenced by the variation of the thermal–conductivity parameter S^*. On the contrary, the temperature profile and the Nusselt number vary with S^*, and these variations are shown in Figs. 16 and 17 for $Mn = 0.40$ and $\Theta_r = -0.50$. From Figs. 16 and 17, it can also be observed that the

Fig. 14. Variations of the dimensionless velocity profile $F'(\xi, \eta)$ with the dimensionless distance η at $\xi = 0.24$ and for zero, positive, and negative values of the magnetic number Mn.

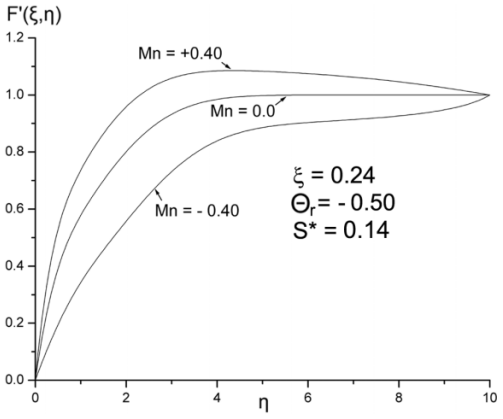

Fig. 15. Variations of the dimensionless temperature profile $\Theta(\xi, \eta)$ with the dimensionless distance η at $\xi = 0.24$ and for zero, positive, and negative values of the magnetic number Mn.

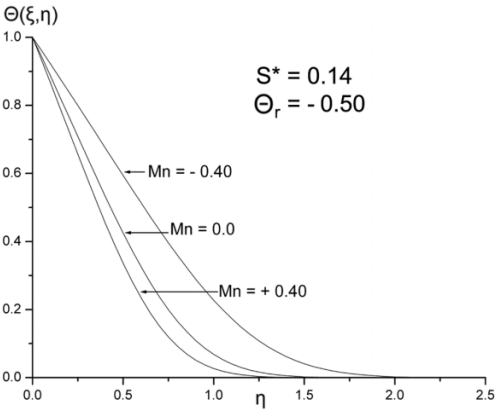

Fig. 16. Variations of the dimensionless Nusselt number Nu_x with the dimensionless distance ξ for different values of the thermal–conductivity parameter S^*.

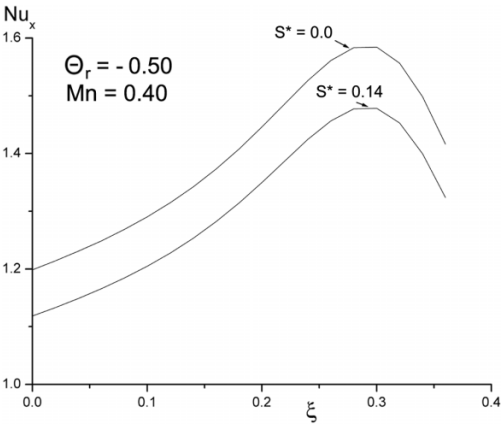

influence of the thermal–conductivity parameter S^* on the Nusselt number is more evident than the corresponding one on the temperature profile.

Fig. 17. Variations of the dimensionless temperature profile $\Theta(\xi, \eta)$ with the dimensionless distance η at $\xi = 0.24$ and for different values of the thermal–conductivity parameter S^*.

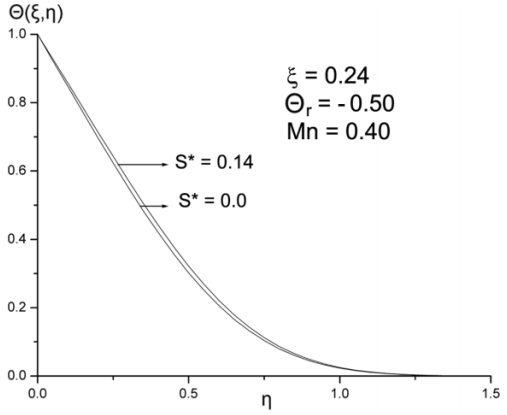

5. Conclusions

In this work, the two-dimensional steady and laminar free-forced convective boundary-layer flow of a biomagnetic fluid over a semi-infinite vertical hot plate was numerically investigated. The flow of the biomagnetic fluid is subjected to the action of a localized magnetic field generated by an electric current going through an infinite thin wire placed parallel to the plate. The equations of the problem were solved by applying an efficient numerical solution scheme. Numerical calculations were carried out, for the case of blood, and the analysis of the results obtained showed that this type of problem could be interesting for medical and bioengineering applications. The important results of the problem under consideration are summarized as follows.

1. The dimensionless skin friction coefficient C_{f_x} and the dimensionless heat transfer coefficient Nu_x are influenced by the presence of the magnetic field, especially in the region where the magnetic source is located ($\xi = 0.331$). This influence is more evident for large values of the magnetic number Mn.

2. The effect of increasing the sensitivity of viscosity to temperature through the parameter Θ_r is different for C_{f_x} and Nu_x. The skin friction coefficient is everywhere increased as $|\Theta_r|$ increases, whereas the Nusselt number decreases as $|\Theta_r|$ increases.

3. At every place along the vertical plate, for example, for every value of ξ, as the magnetic number Mn increases, the velocity profile increases whereas the temperature profile decreases. These profiles present exactly the same dependence on the viscosity–temperature parameter Θ_r.

4. The dimensionless skin friction coefficient C_{f_x} and the dimensionless heat transfer coefficient Nu_x take their maximum or minimum values for a value of ξ that is just before the point $\xi = \xi_0$.

5. When $Mn < 0$, the effect of the magnetic number Mn on the flow field, is different, both qualitatively and quantitatively, with respect to that in the opposite case ($Mn > 0$).

6. The velocity field and the skin friction coefficient are not appreciably influenced by the variation of the thermal–conductivity parameter S^*.

7. The temperature profile and the Nusselt number vary with S^*. The influence of the thermal–conductivity parameter S^* on the Nusselt number, though, is more evident than the corresponding one on the temperature profile.

Acknowledgement

The authors are grateful to the Referee and the Associate Editor for a number of very useful remarks that contributed to the improvement of the paper. ET was supported by the Greek State Foundation of Scholarships (I.K.Y), contract No. 592.

References

1. R.L. Bailey. J. Magn. Magn. Mater. **39**, 178 (1983).
2. A.C. Eringen and G. A. Maugin. Electrodynamics of continua II: Fluids and complex media. Springer, NY. 1990.
3. J. Plavins and M. Lauva. J. Magn. Magn. Mater. **122**, 349 (1993).
4. E.K. Ruuge and A.N. Rusetski. J. Magn. Magn. Mater. **122**, 335 (1993).
5. V. Badescou, O. Rotariu, V. Murariu, and N. Rezlescu. IEEE Trans. Magn. **33**, 4439 (1997).
6. Y. Haik, V. Pai, and C.J. Chen. J. Magn. Magn. Mater. **194**, 254 (1999).
7. C.B. Fuh, L.Y. Lin, and M.H. Lai. J. Chromatogr. A, **874**, 131 (2000).
8. J.M.R. Carlton, C.A. Yowell, K.A. Sturrock, and J.B. Dame. Exp. Parasitol. **97**, 111 (2001).
9. P.A. Voltairas, D.I. Fotiadis, and L.K. Michalis. J. Biomech. **35**, 813 (2002).
10. R. Ganguly, A.P. Gaind, S. Sen, and I.K. Puri. J. Magn. Magn. Mater. **289**, 331 (2005).
11. T. Higashi, A. Yamagishi, T. Takeuchi, N. Kawaguchi, S. Sagawa, S. Onishi, and M. Date. Blood, **82** , 1328 (1993).
12. L. Pauling and C.D. Coryell. Proc. Nat. Acad. Sci. U.S.A. **22**, 210 (1936).
13. Y. Haik, V. Pai, and C.J. Chen. *In* Fluid dynamics at interfaces. *Edited by* W. Shyy and R. Narayanan. Cambridge University Press, Cambridge, UK. 1999.
14. M. Motta, Y. Haik, A. Gandhari, and C.J. Chen. Bioelectrochem. Bioenerg. **47**, 297 (1998).
15. Y. Haik, J.C. Chen, and V.M. Pai. *In* Development of bio-magnetic fluid dynamics. *Edited by* N.E. Wijeysundera. Proceedings of the IX International Symposium on Transport Properties in Thermal Fluids Engineering, Singapore, 25–28 June, Pacific Center of Thermal Fluid Engineering, Hawaii, USA. pp. 121–126.
16. Y. Haik, C.J. Chen, and J. Chatterjee. J. Visualization, **5**, 187 (2002).
17. G.R. Zendehbudi and M.S. Moayeri. J. Biomech. **32**, 959 (1999).
18. H.I. Anderson, R. Halden, and T. Glomsaker. J. Biomech. **33**, 1257 (2000).
19. V.G. Bashtovoy, B.M. Berkovsky, and A.N. Vislovich. Introduction to thermomechanics of magnetic fluids. Hemisphere Publishing Co., Springer-Verlag, Berlin. 1988.
20. B. Berkovski and V. Bashtovoy. Magnetic fluids and applications handbook. Begell House Inc., NY. 1996.

21. E. Blums, A. Cebers, and M.M. Maiorov. Magnetic Fluids. Walter de Gruyter, Berlin, Germany. 1997.
22. V.E. Fertman. Magnetic fluids guidebook: properties and applications. Hemisphere Publishing Co., NY. 1990.
23. R.E. Rosensweig. Annu. Rev. Fluid Mech. **19**, 437 (1987).
24. J.L. Neuringer and R.E. Rosensweig. Phys. Fluids, **7**, 1927 (1964).
25. R.E. Rosensweig. Ferrohydrodynamics. Cambridge University Press, Cambridge, UK. 1985.
26. J.L. Neuringer. Int. J. Non-Linear Mech. **1**, 123 (1966).
27. L.J. Crane. J. Appl. Math. Phys (ZAMP), **21**, 645 (1970).
28. B. Siddappa and B.S Khapate. Rev. Roum. Sci. Techn. Mech. Appl. **21**, 497 (1976).
29. T.C. Chiam. J. Appl. Math. Phys (ZAMP), **62**, 565 (1982).
30. H.I. Andersson and B.S. Dandapat. Stability Appl. Anal. Cont. Media. **1**, 339 (1991).
31. K.B. Pavlov. Magn. Gidrodin. **4**, 146 (1974).
32. H.I. Andersson. Acta Mech. **95**, 227 (1992).
33. H.I. Andersson, K.H. Bech, and B.S. Dandapat. Int. J. Non-Linear Mech. **27**, 929 (1992).
34. H.I. Andersson and O.A. Valnes. Acta Mech. **128**, 39 (1998).
35. E. Tzirtzilakis and N. Kafoussias. J. Appl. Math. Phys (ZAMP), **54**, 551(2003).
36. A.S. Arrot, B. Heinrich, and T.L. Templeton. IEEE Trans. Magn. **25**, 4364 (1989).
37. V.C. Loukopoulos and E.E. Tzirtzilakis. Int. J. Eng. Sci. **42**, 571 (2004).
38. E.E. Tzirtzilakis, V.D. Sakalis, N.G. Kafoussias, and P.M. Hatzikonstantinou. Int. J. Numer. Methods Fluids, **44**, 1279 (2004).
39. E.E. Tzirtzilakis, M. Xenos, V.C. Loukopoos, and N.G. Kafoussias. Int. J. Eng. Sci. **44**, 1205 (2006).
40. E.E. Tzirtzilakis and G.B. Tanoudis. Int. J. Numer. Methods Heat Fluid Flow, **13**, 830 (2003).
41. E.E. Tzirtzilakis. Phys. Fluids, **17**, 077103 (2005).
42. H. Matsuki, K. Yamasawa, and K. Murakami. IEEE Trans. Magn. **13**, 1143 (1977).
43. Y. Haik, V. Pai, and C.J. Chen. J. Magn. Magn. Mater. **225**, 180 (2001).
44. J.X. Ling and A. Dybbs. Forced convection over a flat plate submerged in a porous medium. Paper 87-WA/HT-23, ASME, New York. 1987.
45. J.C. Slattery. Momentum energy and mass transfer in continua. McGraw-Hill, NY. 1972.
46. A.S. Ahuja and W.R. Hendee. Phys. Med. Biol. **23**, 937 (1978).
47. N.G. Kafoussias, D.A.S. Rees, and J.E. Daskalakis. Acta Mech. **127**, 39 (1998)
48. N.G. Kafoussias and E.W. Williams. Int. J. Numer. Methods Fluids, **17**, 145 (1993)
49. J. Daskalakis. Can. J. Phys. **70**, 1252 (1992).
50. J. Daskalakis. Int. J. Energy Res. **17**, 689 (1993).
51. T. Cebeci and P. Bradshaw. Physical and computational aspects on convective heat transfer. Springer-Verlag Inc., NY. 1984. pp. 267, 268, 280, 281, and 467.
52. A. Bejan. Heat convection transfer. J. Wiley and Sons, NY. 1984.
53. J.N. Mazudmar. Biofluid mechanics. World Scientific Publishing Co., Singapore. 1992.
54. J.W. Valvano, S. Nho, and G.T. Anderson. J. Biomech. Eng. **116**, 201 (1994).
55. J.C. Chato. J. Biomech. Eng. **102**, 110 (1980).
56. N.G. Kafoussias and E.W. Williams. Acta Mech. **110**, 123 (1995).

List of symbols

c_p	Specific heat at constant pressure ($J\,kg^{-1}\,K^{-1}$)
C_{f_x}	Local skin friction coefficient
$F(\xi, \eta)$	Dimensionless stream function
$\boldsymbol{H}$	Magnetic field ($A\,m^{-1}$)
g	Gravitational acceleration ($m\,s^{-2}$)
Gr_x	Local Grashof number
k	Thermal conductivity of the fluid ($J\,m^{-1}\,s^{-1}\,K^{-1}$)
k_∞	Thermal conductivity of the fluid in the free stream
$\boldsymbol{M}$	Magnetization of the fluid ($A\,m^{-1}$)
Mn	Magnetic parameter
Nu_x	Local Nusselt number
$Oxyz$	Cartesian coordinate system
$O\xi\eta$	Transformed and dimensionless coordinate system
Pr	Prandtl number
q_w	Wall heat flux ($J\,m^{-2}\,s^{-1}$)
Re_x	Local Reynolds number
S^*	Thermal/conductivity parameter
T	Fluid temperature inside the boundary layer (K)
$T_r = T_\infty - 1/\gamma$	Constant
T_w	Temperature of the plate (K)
T_∞	Free stream fluid temperature (K)
u	Fluid velocity component in x-direction ($m\,s^{-1}$)
u_∞	Free stream fluid velocity ($m\,s^{-1}$)
x	Streamwise coordinate (m)
y	Transverse coordinate (m)

Greek

$\alpha = \gamma/\mu_\infty$	Constant
β	Coefficient of thermal expansion of the fluid (K^{-1})
γ	Thermal property of the fluid (constant)
ϕ	Human blood haematocrit (constant)
ρ_∞	Free stream fluid density ($kg\,m^{-3}$)
τ_w	Wall shear stress ($kg\,m^{-1}\,s^{-2}$)
μ	Dynamic viscosity of the fluid ($kg^{-1}\,s^{-1}$)
μ_∞	Dynamic viscosity of fluid in the free stream ($kg\,m^{-1}\,s^{-1}$)
μ_0	Magnetic permeability ($kg\,m\,A^{-2}\,s^{-2}$)
ν	Kinematic viscosity ($m^2\,s^{-1}$)
ν_∞	Kinematic viscosity in the free stream ($m^2\,s^{-1}$)
$\Theta(\xi, \eta)$	Dimensionless temperature
Θ_r	Viscosity–temperature parameter
υ	Fluid velocity component in y-direction ($m\,s^{-1}$)
χ	Magnetic susceptibility of the fluid (constant)